

© 2015 IEEE. Personal use of this material is permitted. Permission from IEEE must be obtained for all other uses, in any current or future media, including reprinting/republishing this material for advertising or promotional purposes, creating new collective works, for resale or redistribution to servers or lists, or reuse of any copyrighted component of this work in other works.

Title: A Method for Automatic Three-Dimensional Reconstruction of Ice Sheets by Using Radar Sounder and Altimeter Data

This paper appears in: IEEE Journal of Selected Topics in Applied Earth Observations and Remote Sensing (J-STARS)

Date of Publication: 2017

Authors: Ana-Maria Ilisei, Lorenzo Bruzzone

Volume:

Page(s):

DOI: 10.1109/JSTARS.2017.2787199

A Method for Automatic Three-Dimensional Reconstruction of Ice Sheets by Using Radar Sounder and Altimeter Data

Ana-Maria Ilisei, *Member, IEEE*, and Lorenzo Bruzzone, *Fellow, IEEE*

Abstract—Understanding the processes occurring at the ice sheets requires reliable 3D models of the ice sheet geometry. To address this challenge, we propose a technique for the 3D reconstruction of the ice sheet geometry that uses Radar Sounder (RS) and altimeter (ALT) data to automatically identify the scale (or grid size) for interpolation. Existing studies derive the interpolation scale empirically, by qualitatively analyzing the RS data sampling and often neglecting the surface topography effects. Our method initially performs the interpolation of RS data at several potential scales. At each scale it uses the ordinary kriging interpolation method which enables the quantitative analysis of both the RS data sampling and the surface topography. The optimal scale for the estimation of the surface map is identified according to an objective criterion that minimizes the difference to a subset of reference ALT data. Thereafter, the identified optimum scale on the surface is used to estimate the bedrock and ice thickness maps. Thus, the technique is a best-effort approach to the reconstruction of the ice sheet geometry given the reference surface data and in the absence of reference bedrock data. Results obtained by applying the method to RS and ALT data acquired over the Byrd Glacier in Antarctica, in four regions characterized by different RS sampling and surface topography, confirm its effectiveness. Moreover, they point out that the method could be used for guiding future RS surveys, since the identified optimal scales are typically larger than those needed for addressing specific science objectives.

Index Terms—3D reconstruction, ice sheet, radar sounder, altimeter, remote sensing

I. INTRODUCTION

RELIABLE maps of the ice surface, bedrock and ice thickness are fundamental in several glaciological applications, e.g., ice mass balance computation [1], ice flow modeling [2], geophysical data interpretation [3], land stability evaluation [4] and sea level rise projection [5]. Remote sensing data acquired at the ice sheets are the main input for the generation of such maps. In particular, radar sounder (RS) instruments, which acquire radargrams that show the ice sheet cross-section (ice surface, thickness and bedrock elevation), and altimeters (ALT), which acquire surface elevation data, represent two of the most rich sources of information suitable for the large-scale analysis of the ice sheet surface and/or subsurface. RSs are usually operated on airborne platforms. During the many RS airborne campaigns carried out, a huge volume of RS data with heterogeneous quality, spatial resolution and regional coverage has been generated and is now available in archives. ALTs are laser or radar instruments that can be operated on both airborne and satellite platforms. Thus, in the past decades ALTs have provided enormous quantities

of ice surface elevation data. The availability of RS and ALT data and the need for a reliable 3D reconstruction of the ice sheets call for the development of automatic techniques that can make efficient use of such data (see Sec. II).

The literature on the development of automatic techniques for the reliable reconstruction of the ice sheet geometry is still limited. Two methods to map the global 3D structure of Antarctica are presented in [6] and [7], whereas [8] and [9] present techniques for mapping the ice geometry of Greenland. All these methods consider most of the available data acquired in Antarctica or Greenland at the time of their publication. Such data are extremely heterogeneous in terms of resolution and sample density, since they were acquired in different airborne campaigns conducted to meet different science requirements. However, the 3D maps are generated at a common single scale (or grid size) determined by empirically analyzing the global density of the data at hand. This choice has two potential drawbacks. In regions with high data sampling density, the use of relatively large scales determines the generation of low resolution maps, leading to possible loss of information. On the contrary, in regions with low data sampling density, the use of relatively small scales determines the generation of elevation maps with artifacts or artificial features. In [10], the scale used to interpolate the RS data is also chosen empirically, based on the sampling of the data. Then, high-resolution maps of a land-terminating section of the Greenland ice sheet are generated with the universal kriging method. In [11], the bedrock topography is estimated regionally, i.e., for the Jakobshavn Isbrae in Greenland and Byrd Glacier in Antarctica. The work focuses on the description of a novel RS system used for data acquisition in these regions and emphasizes on its capability to reach the bedrock even under very thick ice ($\approx 3\text{km}$) below the flightlines. However, it lacks a detailed description of the methods used to identify the scale and of the interpolation strategy used to reconstruct the 3D structure of the ice sheet. In [12], the authors propose a physically-based approach to calculate glacier ice thickness by using a dynamic model to obtain spatially distributed thickness of individual glaciers. The method uses two types of data, i.e., a complete inventory of glacier outlines and digital elevation models (DEMs). It calculates glacier-specific distributed thickness based on the inversion of surface topography by using the principles of ice flow dynamics. The same method is further developed and adapted to glaciers on the Antarctic Peninsula in [13]. Another physically-based approach to the interpolation of ice thickness of the Aurora Subglacial Basin

is presented in [14]. The method is a development of that used in [15] and makes extensive use of the surface topography to define down slope streamlines along which the interpolation is performed. In [16], the basal topography of Bayley/Slessor region of East Antarctica is obtained by interpolating RS data with the kriging method. A mass conservation approach to map the glacier ice thickness, which exploits RS and interferometric synthetic aperture radar data, is presented in [17] and further improved in [18] for the high-resolution ice thickness mapping in South Greenland. This review of the related literature points out that there are several interpolation methods used for the same purpose, i.e., 3D estimation of ice thickness and bedrock topography. However, it is worth noting that independently of the interpolation method used, the above-mentioned techniques use empirically-derived scales for interpolation. For instance, in [16], [6], [13], the scales used are 20km, 5km, 100m, respectively. In [16] the authors state that the choice of an interpolation scale of 20km for the reconstruction of the Bayley/Slessor region of East Antarctica can be considered an acceptable compromise, given the extremely different sampling of the RS instrument in the horizontal direction, i.e., 25m in the along-track direction and about 40km in the across-track direction. In [6], the choice of a scale of 5km for the 3D reconstruction of the whole Antarctica is motivated by the fact that 5km appears to be sufficient to resolve ice streams and major outlet glaciers. However, the authors observed that although there are regions with sufficient sampling to justify a scale of 5km, there are also wide regions not sufficiently sampled to support the choice of such a fine scale. Therefore, these values represent an acceptable trade-off choice given the different sampling of the data versus the scales desired for specific science objectives. For instance, a scale of about 5km is sufficiently accurate to describe inland regions [19]; a kilometric scale is required for describing coastal outlet glaciers and capturing channelized landscapes [20], [19]; the maximum bound on the scale of interpolation has still to be assessed for accurately simulating ice-sheet dynamics [21]. However, none of the scales chosen in the aforementioned works has been automatically identified by analyzing objectively and quantitatively the sampling of the data. Moreover, these scales have not been chosen by analyzing the elevation variability of the surfaces. In fact, it is likely that surfaces with different topography but similar RS sampling can be reliably reconstructed at different scales. These issues have been marginally addressed in the literature, thus calling for the development of efficient techniques that can reconstruct the ice sheet at an optimal scale, i.e., a scale that can be automatically derived by taking into account both the characteristics of the ice sheet and the sampling of the available RS data.

In this paper we present a technique for the 3D reconstruction of the ice sheets, which uses RS and ALT data for the automatic identification of the scale for interpolation. In particular, it uses the RS data for the 3D reconstruction and the ALT data, which is split into two distinct datasets, as reference for scale selection and validation. The technique aims to address two main challenges: i) the reconstruction should be performed by interpolating the RS data at a scale

derived automatically on the basis of an objective criterion, and ii) the reconstruction should have the highest overall quality, i.e., the lowest overall uncertainty. To address these challenges, we employ the ordinary kriging (OK) method [22], which analyzes the topography variability of the investigated surfaces at the sampling of the RS data, and provides both estimated 3D elevation maps of the surface and bedrock, along with uncertainty maps that quantify the overall quality of the estimation. The presented method relies on data processing techniques and objective statistical measures for the automatic identification of the scale for interpolation, hereafter denoted s^* . It is composed of four main steps, i.e., A) RS data preprocessing, B) automatic identification of the optimal scale of the ice surface and estimation of the ice surface map, C) estimation of the bedrock map, and D) estimation of the ice thickness map. The first step extracts the surface and bedrock elevation from the RS data. The second step interpolates the ice surface RS data at several potential scales using the OK technique and identifies the optimal scale based on a criterion that minimizes the overall error between the interpolated maps and a subset of the ALT data. Similarly, the optimal scale is also validated by using a second subset of the ALT data. In the third step, in the absence of reference data of the bedrock, the identified optimal scale of the ice surface is used to interpolate the bedrock RS data for the estimation of the bedrock elevation map. Finally, in the fourth step, the ice thickness map is generated by subtracting the estimated surface and bedrock elevation maps. As it will be shown, since the identified scale is optimal for the interpolation of the surface, whereas it is presumably suboptimal for the interpolation of the bedrock RS data, the method shall be regarded as a best-effort approach to the reconstruction of the ice sheet geometry based on the availability of reference data on the surface and absence of reference data on the bedrock.

The main novelty and advantage of the technique is that it identifies the optimal scale automatically based on a quantitative analysis of both the surface topography variability and the RS sampling. This is important for two main reasons, i.e., i) it provides an objective criterion for identifying the lower bound of the scale for interpolation by proving that empirical attempts to choose lower scales yield higher overall errors and potentially introduce artifacts in the reconstruction, and ii) it provides guidelines for defining the density of RS surveys in relation to the requirements on the scale needed for a given science objective. Additionally, the joint use of the RS and ALT data for the automatic identification of the optimal scale on the surface, as well as the analysis and use of the uncertainty maps generated by the OK method, are notable enhancements relative to previous literature methods, e.g., [9], [16].

The method has been applied to RS data acquired by the MultiChannel Coherent Radar Depth Sounder (MCoRDS) [23] and ALT data acquired by the Geoscience Laser Altimeter System (GLAS)/ICESat [24] over a large portion ($\approx 200 \times 200$ km) of the Byrd Glacier in Antarctica. In particular, to prove the effectiveness of the method for the reconstruction of the ice sheet and for the automatic identification of the scale for interpolation, it has been applied to four regions of

Byrd Glacier, which are different in terms of area, surface topography variation and RS sampling. The results confirm the usefulness of the automatic identification of the scale, i.e., for the different regions analyzed, the presented method provides different scales which are qualitatively consistent with the ice surface variability and the sampling of the data, and are quantitatively confirmed by validation with a second subset of ALT data.

The rest of the paper is organized as follows. Sec. II describes the main properties of the RS and ALT data. The technique (which relies on the OK method, see Appendix A) is presented in details in Sec. III. Sec. IV illustrates and discusses results obtained by applying the technique to RS and ALT data acquired in Antarctica. Finally, Sec. V draws the conclusion of this work and proposes ideas for future developments.

II. PROPERTIES OF RADAR SOUNDER AND ALTIMETER DATA ACQUIRED OVER THE ICE SHEETS

There are several archives containing both RS and ALT data acquired at the ice sheets. In this section we describe their general properties, mainly in terms of coverage and sampling. *Radar sounder data.* RS data, or radargrams, contain georeferenced vertical profiles of the ice sheet. They are acquired during dedicated airborne campaigns at the ice sheets [shown schematically in Fig. 1(a)]. RS systems that have been used to obtain data on the ice sheets include MultiChannel Coherent Radar Depth Sounder (MCoRDS) [23], High Capability Radar Sounder (HiCARS) [25], POLarimetric Airborne Radar Ice Sounder (POLARIS) [26]. At present, because of frequency allocation and physical constraints, there are no satellite-mounted RSs for Earth observation. Due to the nature of airborne surveys, RS data typically have inhomogeneous quality, coverage and resolution. Science requirements and technological constraints drive data acquisition strategy plans (e.g., location, coverage) and condition the data quality (e.g., maximum penetration, resolution). Therefore, the RS data acquired during different campaigns present different properties. Nonetheless, there are properties of the RS data that are common in most acquisitions. For instance, the spacing between two adjacent measurements in the flightline (along-track/azimuth) direction d_x^{RS} is typically much smaller than the spacing between two adjacent flightlines (across-track direction) d_y^{RS} (see Fig. 1). This results in a highly irregular sampling pattern in the horizontal direction [see Fig. 1(b)], with d_x^{RS} (in the order of few m) \ll d_y^{RS} (few hundreds of m to tens of km). Depending on the planning of the campaign, the spacing between adjacent flightlines can be uniformly small (1km or less), moderate (few km, e.g., see the sampling of Jakobshavn Isbrae in Greenland in [11]) or large (tens of km, e.g., see the sampling of Bayley/Slessor in [16]), or it can be variable in different portions of an investigated area (e.g., see the sampling of Byrd Glacier in Antarctica in [11]).

Altimeter data. Contrary to RS systems that acquire georeferenced 2D vertical profiles of the ice sheet subsurface, ALTs take georeferenced measurements of the ice surface elevation only. Such measurements can be acquired both from airborne and satellite platforms. Often, during the airborne campaigns,

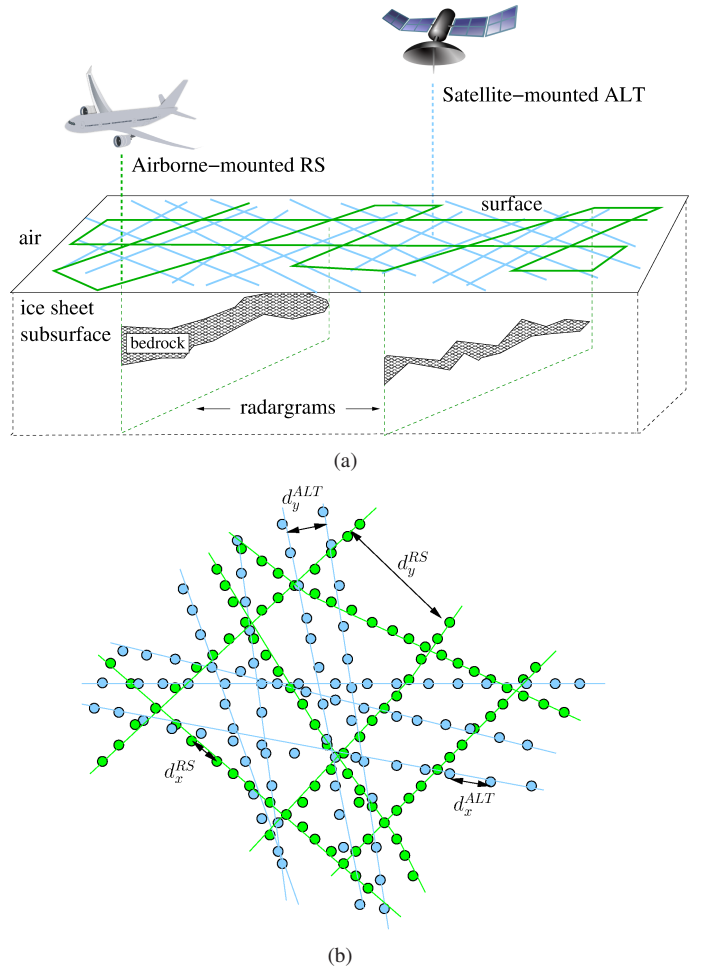


Fig. 1. Schematic representation of airborne-mounted RS and satellite-mounted ALT data (a) acquisition and (b) sampling over the ice sheets. Note that the RS and ALT data are not acquired exactly on the same ground tracks.

both RS and ALT data are acquired at the same time, on the same ground tracks, thus the coverage and the horizontal sampling of the ALT are comparable to that of the RS. The situation is different in the case of satellite missions during which ALTs acquire data with a more uniform coverage on tracks that are not necessarily overlapped on those of the RS (see Fig. 1). The horizontal sampling of the ALT in terms of spacing between adjacent samples d_x^{ALT} and adjacent tracks d_y^{ALT} shows an irregular pattern similar to that of the RS, with $d_x^{ALT} < d_y^{ALT}$ [see Fig. 1(b)].

The above analysis points out that airborne-mounted RS data and satellite-mounted ALT data have complementary sampling attributes which enable the joint use of the two types of data for the reliable reconstruction of the ice sheet geometry. In particular, we propose (see Sec. III) the interpolation of the RS data for generating ice surface and bedrock 3D maps, and the use of the satellite ALT data for the identification and validation of the scale for interpolation on the surface.

III. PROPOSED METHOD

The technique is made up of four main steps (see Fig. 2) and relies on the use of the OK method. The motivation for this

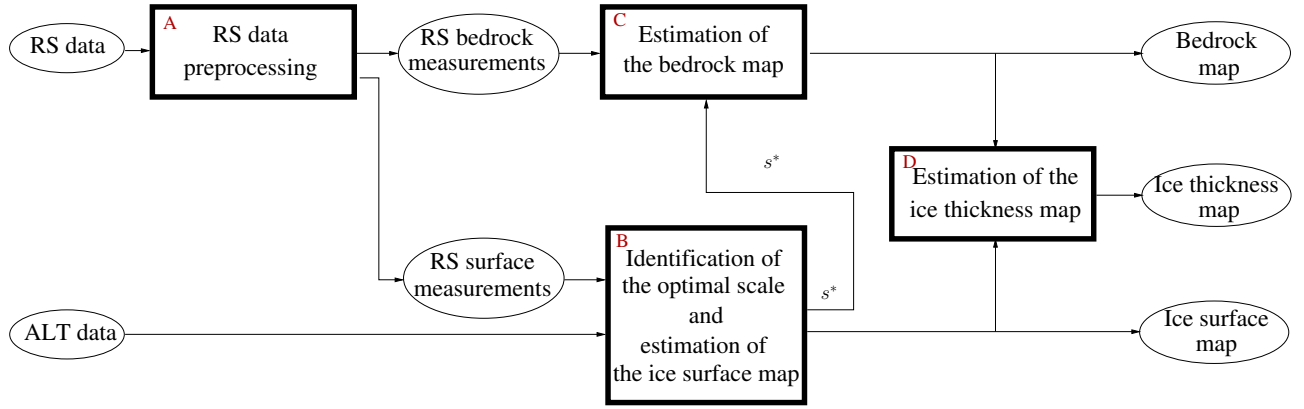


Fig. 2. Block scheme of the technique. A detailed flowchart of step B is given in Fig. 3.

choice is given by the intrinsic properties of the OK method, i.e., i) it analyzes the variability of the surfaces prior to the interpolation, and ii) it generates uncertainty maps along with the estimated interpolated maps (for details on the OK method, see Appendix A). A detailed description of all the processing steps of the method is given in the following subsections.

A. RS data preprocessing

The aim of this step is the extraction from the radargrams of the surface and bedrock elevation along the flightline direction at the original scale s_0^{RS} of the RS data. We define s_0^{RS} as the spacing between two adjacent measurements (or columns/traces of the radargram) in the along-track direction, i.e., $s_0^{RS} = d_x^{RS}$. Each trace of the radargram contains the RS measurements of power reflected by the surface and subsurface features at each platform coordinate in the azimuth direction as a function of radar wave two-way travel time. We first detect the surface and bedrock reflection positions. This can be done manually or according to automatic techniques [27]. Then, we estimate the elevation of the ice surface and bedrock for all traces of the radargram by using the elevation of the platform (given along with the radargram) and a standard time-distance conversion equation that considers propagation in two media, air and ice. The output of this step consists of two sets of measurements forming an irregular pattern, i.e., the surface elevation and the bedrock elevation at the initial along-track scale s_0^{RS} of the RS data, i.e., $S^{RS}(s_0^{RS})$ and $B^{RS}(s_0^{RS})$, respectively. The set $S^{RS}(s_0^{RS})$ is used in the second block of the technique (see Sec. III-B and Fig. 3), whereas the set $B^{RS}(s_0^{RS})$ is used in the third step (see Sec. III-C).

It is worth mentioning here that there are a few factors that influence the accuracy of the above estimations. Clutter is one critical factor. It is due to off-nadir surface reflections arriving at the RS receiver at the same time as the nadir reflections from the subsurface. For this reason, the clutter may mask the bedrock reflection. In order to limit the negative effect of clutter on the estimation of the ice thickness, we use radargrams processed with the minimum variance distortionless response algorithm for clutter reduction [28]. Other errors in the estimation of the ice elevation and thickness are due to the accuracy of the global positioning system, the sampling

frequency of the RS in the vertical direction, the accuracy of the automatic detection method employed and the assumed dielectric permittivity of the ice. In fact, we here consider a constant dielectric permittivity of pure ice $\varepsilon_r^{ice} = 3.15$ along the whole ice column, neglecting the presence of firm and ice impurities. However, this can result in less than 10m of error in the ice thickness estimate [11].

B. Automatic identification of the optimal scale and estimation of the ice surface map

This step aims to identify the optimal scale s^* at which the irregular pattern of ice surface elevation samples $S^{RS}(s_0^{RS})$ should be interpolated. The identification of the optimal scale is performed automatically based on an objective statistical measure that involves the use of a subset of the reference ALT data. Moreover, the method aims to estimate the ice surface map that has the highest overall quality across different OK parameter sets (see Appendix A). To address these challenges, we investigate a) several potential candidate scales $s_j, j = [1..J]$, and b) for each candidate scale s_j several parameter sets $p_i^S, i = [1..P]$. As depicted in Fig. 3, this is accomplished in 3 main sub-steps: 1) Processing of the surface elevation from the ALT data, 2) Processing of the surface elevation from the RS data, and 3) Parameter set and scale selection.

1) *Processing of the surface elevation from the ALT data:* As already mentioned, the ALT data provide only the ice surface elevation and are used by the method as reference for identifying, and subsequently for validating, the scale for the interpolation of the RS data. We collect these data in a set of measurements $S^{ALT}(s_0^{ALT})$, where s_0^{ALT} is the original scale of the ALT data, defined as the spacing between two adjacent measurements in the the along-track direction, i.e., $s_0^{ALT} = d_x^{ALT}$. Since for the interpolation we are investigating several candidate scales, the ALT data used as reference should be available at the same scales $s_j, j = [1..J]$. Thus, in this step we are generating J sets of ALT data at different scales s_j by averaging adjacent measurements of the original ALT data on a distance s_j . Note that by doing so, we aim to capture the significant trend of the data at each investigated scale and remove unnecessary details. Then, at each scale we generate two subsets of rescaled ALT data. Each subset contains a

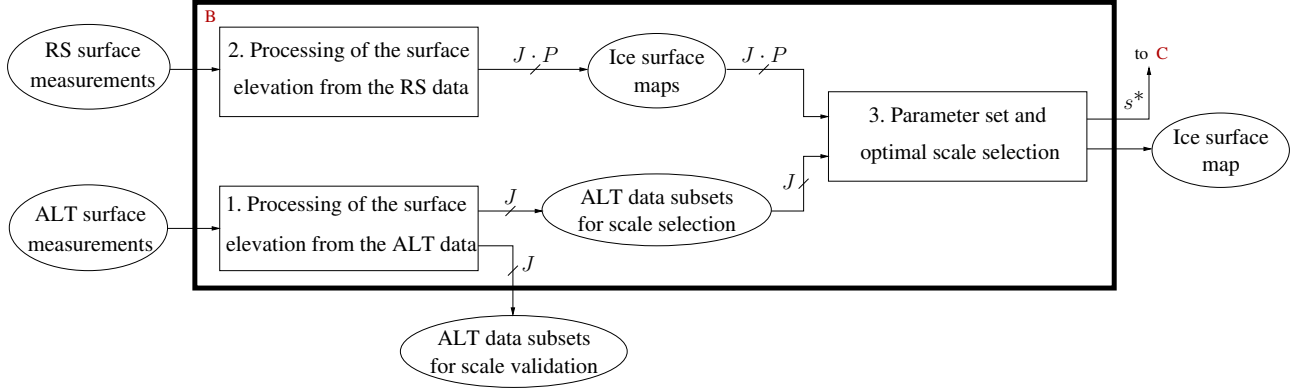


Fig. 3. Flowchart of the second step of the technique, i.e., step B in Fig. 2.

statistically significant number of randomly selected samples from the rescaled ALT data. The obtained samples, i.e., for each subset 10% of the total of rescaled ALT samples, are collected in $S_I^{ALT}(s_j)$ and $S_V^{ALT}(s_j), \forall j = [1..J]$, representing two different ALT subsets used for scale identification and scale validation, respectively (see Sec. III-B3 and Fig. 3).

2) *Processing of the surface elevation from the RS data:*

The final goal of this step is the estimation of the set of surface elevation maps obtained by applying the OK method with P different parameter sets at a generic scale s_j . To this end, we use the available surface elevation measurements $S^{RS}(s_0^{RS})$ (see Sec. III-A). Since we are interested in the results at scale s_j , we first rescale $S^{RS}(s_0^{RS})$ to obtain $S^{RS}(s_j)$. We accomplish this by averaging adjacent RS measurements in the along-track direction on a distance s_j and by collecting one measurement every s_j meters. The rescaling of the RS data is performed similarly to the rescaling of the ALT data, in order to reduce the details and retain only the significant surface trend at each scale. Note that by increasing s_j , the pattern of these measurements becomes more regular, with the along-track spacing of the rescaled measurements $d_x^{RS}(s_j) = s_j$ approaching d_y^{RS} . Then, we interpolate $S^{RS}(s_j)$ with the OK method (see Appendix A) by considering for the interpolation at each query point its $N_0 = 10$ nearest observed neighbors from $S^{RS}(s_j)$. As there are P possible parameter sets to be used in the OK method (see Appendix A), for each scale s_j the technique generates P couples of ice surface maps $\mathbf{S}_{p_i}^{RS}(s_j)$ and uncertainty maps $\mathbf{U}_{p_i}^S(s_j), i = [1..P]$. From Appendix A, it is worth noting the number of simulations carried out by the OK method for the generation of the P couples of surface and uncertainty maps at a certain scale s_j . Since there are 4 semivariogram models (i.e., Spherical, Exponential, Gaussian and Linear) and $P = 8$ parameter sets that reflect different binning and weighting options of the semivariograms, the number of simulations can be either $32 (= 4 * 8)$ in the case of stationary data, or $56 (= 4 * 8 + 3 * 8)$, because the linear model is excluded in the fitting of the regenerated semivariogram in the case of non-stationary data.

3) *Parameter set and scale selection:* The aim of this step is two-fold, i.e., i) the identification at a generic scale s_j of the parameter set p^{*S} (hereafter called best parameter set) that provides the ice surface elevation map with the highest overall

quality $\mathbf{S}_{p^{*S}}^{RS}(s_j)$, and ii) the identification of the optimal scale s^* and the corresponding surface elevation map $\mathbf{S}_{p^{*S}}^{RS}(s^*)$.

i) The lower the uncertainty value provided by the OK method, the more the estimated value is expected to approach the true value, i.e., the better the estimation (see Appendix A). Therefore, the key idea is to analyze the P uncertainty maps generated by the OK method and to choose the parameter set that minimizes the overall uncertainty (OU) of the maps across parameter sets $p_i, i = [1..P]$. Note that OU, which we define as the mean value of $\mathbf{U}_{p_i}^S(s_j), i = [1..P]$, is an objective criterion which equally treats the estimated uncertainty at all query points. Therefore, by minimizing OU we aim to obtain, at each scale, the map with the lowest overall uncertainty, i.e., with the highest overall quality. This operation provides the best parameter set $p^{*S}(s_j)$ and thus $\mathbf{S}_{p^{*S}}^{RS}(s_j)$. The identification of the best parameter set is performed for all the scales $s_j, j = [1..J]$. Thus, we obtain a set of J elevation maps $\mathbf{S}_{p^{*S}}^{RS}(s_j), j = [1..J]$ with the highest overall quality at each scale.

ii) Then, we identify the optimal scale s^* by minimizing the overall absolute error (OAE) between the estimated surface elevation maps $\mathbf{S}_{p^{*S}}^{RS}(s_j)$ and the reference subset of rescaled ALT samples $S_I^{ALT}(s_j)$ (see Sec. III-B1) across the investigated candidate scales $s_j, j = [1..J]$. The error at a query point at a generic scale s_j , i.e., the error in a grid cell of size s_j , is computed as the difference between the estimated surface elevation value and the average value of the rescaled ALT data in the grid cell. Then OAE is defined as the mean value of the absolute error at all considered grid points. Note that OAE is an objective criterion which equally treats the estimated elevation values at all query points. Therefore, by minimizing OAE across scales we identify the scale that, from a statistical point of view, provides the ice elevation map that best fits the reference ALT samples. This operation provides s^* and thus $\mathbf{S}_{p^{*S}}^{RS}(s^*)$. It is worth noting that, although we identify the best parameter set and the optimal scale based on the minimization of the first order statistics (mean), other criteria could also be used, e.g., based on second order statistics (variance), R^2 indicator, root mean square error.

The scale validation is performed by verifying if the scale obtained by minimizing the OAE between the interpolated surface maps and the ALT validation set $S_V^{ALT}(s_j)$ is equal

to the optimal scale obtained with the proposed method.

C. Estimation of the bedrock map

The processing steps involved in the estimation of the bedrock map are similar to those performed for the estimation of the ice surface elevation map. The main difference is that, in the absence of reference data for the bedrock, we analyze the interpolation results only at scale s^* (see Fig. 2). Thus, we rescale the RS bedrock measurements at s^* in order to obtain $B^{RS}(s^*)$ and interpolate $B^{RS}(s^*)$ with the OK method (see Appendix A) as done with the surface samples. Since the OK method is run with P parameter sets, we obtain a set of P couples of estimated bedrock maps $\mathbf{B}_{p_i}^{RS}(s^*)$ and corresponding uncertainty maps $\mathbf{U}_{p_i}^{\mathbf{B}}(s^*)$, $i = [1..P]$. Then, we select the best parameter set $p^{*\mathbf{B}}$ as the one that minimizes the OU of the estimated bedrock maps. This operation provides $p^{*\mathbf{B}}$ and thus $\mathbf{B}_{p^{*\mathbf{B}}}^{RS}(s^*)$.

Note that according to the criterion used for estimating s^* , using a scale smaller than s^* for the interpolation of the surface RS data determines higher overall absolute errors (see also Sec. IV), besides introducing artifacts. Since i) the bedrock elevation variability is generally higher than that of the surface, and ii) the spatial sampling of the RS data at the bedrock is equal to that at the surface, the abovementioned negative effects would be even more critical for the interpolation of the bedrock RS data at scales smaller than s^* . For this reason and in the absence of reference data of the bedrock, we chose to interpolate the RS bedrock elevation measurements at scale s^* , which has been identified and validated on the surface. Summarizing, the method provides an optimal scale for the estimation of the ice surface map, whereas the scale is coherent and likely suboptimal for the estimation of the bedrock map. Thus, using the scale of the surface to interpolate the measurements of the bedrock is a best-effort approach to reconstruct the ice sheet geometry from the RS data, based on the available reference surface ALT data and in the absence of reference bedrock data. When reference bedrock data will become available (e.g., 3D-bed tomography [29]), the method presented in Sec. III-B3 could be applied in a more rigorous way also to estimate the optimal scale for the generation of the bedrock map.

D. Estimation of the ice thickness map

Once the scale s^* , the surface elevation map and the bedrock elevation map have been derived, the ice thickness map $\Delta^{RS}(s^*)$ can be obtained as:

$$\Delta^{RS}(s^*) = \mathbf{S}_{p^{*\mathbf{S}}}^{RS}(s^*) - \mathbf{B}_{p^{*\mathbf{B}}}^{RS}(s^*). \quad (1)$$

It is worth highlighting that the ice thickness map could be obtained by directly interpolating the thickness measurements extracted from the RS data rescaled at s^* , i.e., by interpolating with the OK method the values $S^{RS}(s^*) - B^{RS}(s^*)$. However, this may introduce more ambiguities in the estimation, which are due to both the surface and bedrock elevation variability. For this reason, we chose to interpolate the bedrock measurements, and to subtract the result from the interpolated surface, to obtain the ice thickness map.

IV. EXPERIMENTAL RESULTS

The described technique has been applied to RS data acquired by MCoRDS [23] and ALT data acquired by GLAS [24] over a large portion ($\approx 200 \times 200$ km) of the Byrd Glacier in Antarctica. Tab. I reports the specific properties of the analyzed data. Fig. 4 shows the investigated portion of the Byrd Glacier. Given the large variability of the surface topography and of the sampling of the RS instrument in different portions of the analyzed area, in order to prove the effectiveness of the described method, we apply it to four distinct regions defined and characterized as follows:

- R1 (red rectangle in Fig. 4) covers an area of 30×30 km with smooth topography and high RS sampling;
- R2 (blue rectangle in Fig. 4) covers an area of 40×40 km with rough topography and moderate RS sampling;
- R3 (magenta rectangle in Fig. 4) covers an area of 80×80 km with variable topography and low RS sampling;
- R4 (black rectangle in Fig. 4) covers an area of 100×100 km with variable topography and variable RS sampling, e.g., low sampling in the top left side and high sampling in the bottom right side.

The ALT and RS measurements over the regions R1, R2, R3 and R4 are shown qualitatively in Fig. 5(a), Fig. 5(b), Fig. 5(c) and Fig. 5(d), respectively.

The largest scale considered in the analysis of each region is bounded by the area of the region and by the minimum number of rescaled RS data required by the OK method in order to provide a meaningful geostatistical analysis inside the region. The smallest scale, i.e., 500m, is the minimum scale considered by previous studies in the Byrd Glacier [11]. Intermediate scales are chosen with a step size of 500m between the minimum and maximum scale in each region. According to these criteria, the candidate scales are:

- R1: $s_j = [500:500:5000]$ m, $J = 10$;
- R2: $s_j = [500:500:5000]$ m, $J = 10$;
- R3: $s_j = [500:500:8000]$ m, $J = 16$;
- R4: $s_j = [500:500:10000]$ m, $J = 20$.

We applied the method to each region independently in order to identify the corresponding optimal scales for the interpolation of the ice surface RS measurements. For the identification of the optimal scales we used the subset of reference ALT data $S_f^{ALT}(s_j)$, $j = [1..J]$ (see Sec. III-B1). Fig. 6 reports the OAE obtained at each candidate scale and the identified optimal scale for each region.

By analyzing together Fig. 5 and Fig. 6 one can derive the following observations:

- Independently on the scale, $OAE(R1) < OAE(R4) < OAE(R2) < OAE(R3)$. The relation $OAE(R1) < OAE(R3)$ is expected given the sampling of the RS data in these regions, i.e., the highest in R1 and the lowest in R3, see Fig. 5(a) and Fig. 5(c), respectively. The relation $OAE(R4) < OAE(R2)$ is likely due to the smoother short range topography of R4 with respect to the topography of R2, see Fig. 5(d) and Fig. 5(b).
- The identified optimal scales are 3000m, 4500m, 7500m and 8500m, for the regions R1, R2, R3 and R4, respectively. This result is summarized qualitatively in

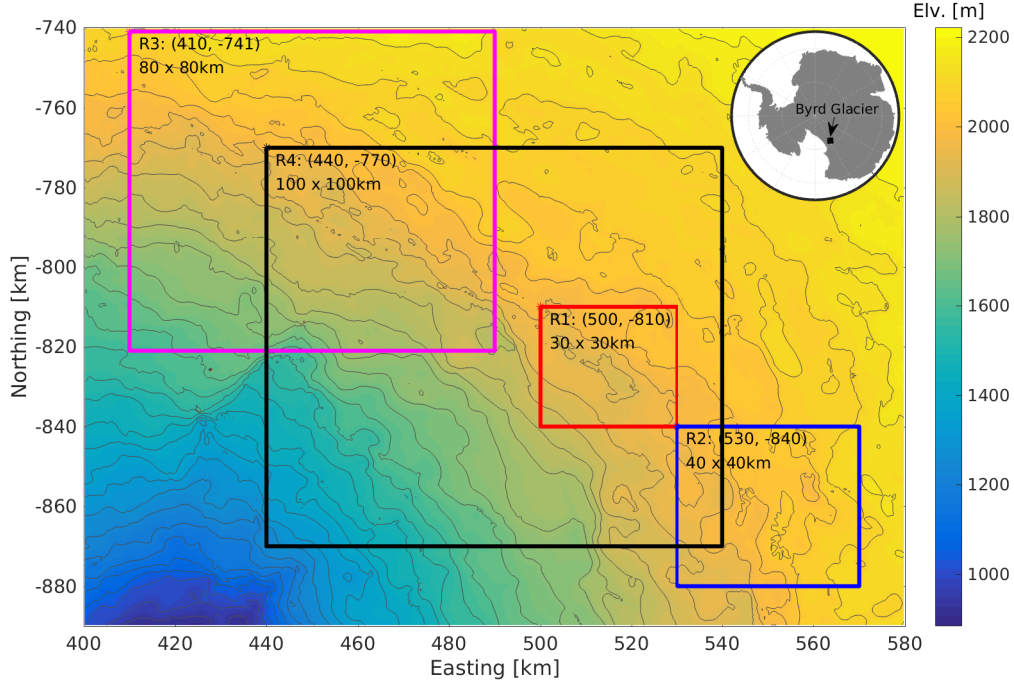


Fig. 4. Investigated portion of the Byrd Glacier in Antarctica. The inset shows the location of Byrd Glacier in Antarctica map. The ice surface DEM is the one provided in [30]. The colored rectangles represent four investigated regions which are different in terms of area, surface topography variation and RS and ALT sampling (see also Fig. 5). The dimension in km and the polar stereographic (70S latitude of true scale) (x,y) coordinates of the top left corner of each region are also illustrated.

TABLE I
PROPERTIES OF THE RS AND ALT DATA USED IN THE EXPERIMENTS.

Property	RS data (MCoRDS)	ALT data (GLAS)
Horizontal spacing	$d_x^{RS} = 15\text{m}$, d_y^{RS} variable	$d_x^{ALT} = 170\text{m}$, d_y^{ALT} variable
Horizontal resolution	$\delta_x^{RS} = 25\text{m}$ with SAR processing, $\delta_y^{RS} \in [35 - 250]\text{m}$ depending on surface roughness (at a platform height $\approx 500\text{m}$)	$\delta_x^{ALT} = \delta_y^{ALT} = 70\text{m}$
Vertical resolution	$\delta_z^{RS} = 4.3\text{m}$ in ice, $\delta_z^{RS} = 7.4\text{m}$ in air with range compression and windowing factor $k_t = 1.53$	$\delta_z^{ALT} = 15\text{cm}$

Fig. 7, which reports the sampling of the RS and ALT instruments over the analyzed portion of the Byrd Glacier and the optimal scale. As one can see by combining the information in Fig. 5 and Fig. 7, the size of the output grid cell, which is derived automatically with the described method, is highly dependent on the sampling of the input RS and ALT data and on the surface topography variation.

- The identified optimum scales, ranging from 3000m to 8500m, depending on the sampling and surface features in each region, are typically larger than those generally needed for certain science requirements, e.g., [19], [20], [21]. These large estimated scale values are due to the scarce sampling in the investigated regions. Indeed, a scarce sampling inevitably misses important details (e.g., resolution of mesoscale channelized morphology to guide glacier flow, resolution of small-scale roughness to determine topographic resistance to flow [20]. In order to be able to improve the optimum interpolation scale to meet specific science applications, it is necessary to plan more

dense RS surveys.

- The errors committed by forcing the interpolation of the surface RS data at scales different from the optimal one can be deduced from Fig. 6. In particular, the differences between the $OAE(s^*)$ and $OAE(s_j \neq s^*)$ range from few centimeters to more than 10m (e.g., on region R3, the OAE is 72m at scale 500m, whereas it is 59m at the optimal scale 7500m). The analysis of these results offers the possibility to perform a quantitative error assessment of the interpolation at scales that match the needs of specific objectives or applications (e.g., ice sheet modeling) but are different from the identified optimal scale. It also enables evaluating the criticality in choosing arbitrarily the scale for interpolation.

Let us focus on the ice sheet reconstruction at the identified scales. Since the procedure is similar for all the analyzed regions, here we provide and discuss the results obtained on region R2, which is characterized by a moderate RS sampling.

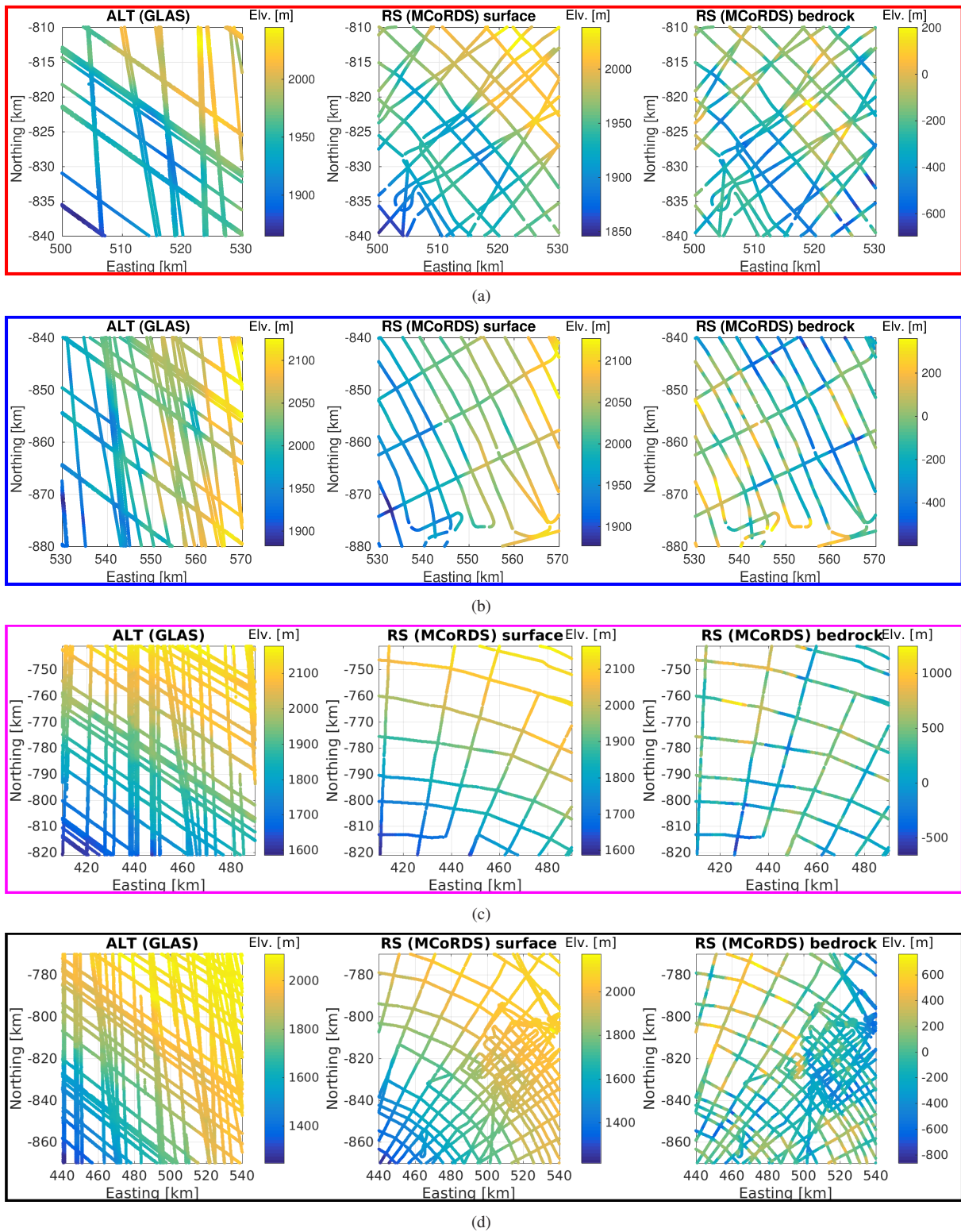


Fig. 5. ALT surface measurements and RS surface and bedrock measurements over the regions (a) R1, (b) R2, (c) R3, and (d) R4.

As described in Sec. III, at all candidate scales, the OK method provides $P = 8$ couples of estimated surface elevation and uncertainty maps, each couple corresponding to a different parameter set. Among these, the estimated surface map with the highest overall quality at each scale is the one generated with the parameter set that provides the minimum overall

uncertainty (OU) across parameter sets. Because of space constraints, here we report the results obtained at the identified optimal scale 4500m on region R2. The variability of the OU across parameter sets is given in Fig. 8. As one can see, the parameter set that minimizes the OU is p_5 . The RS measurements of the surface at scale 4500m and the

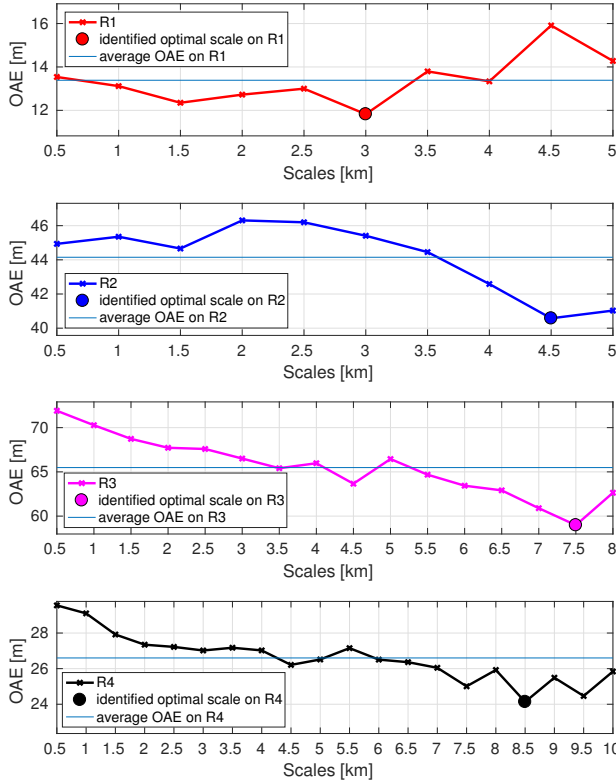


Fig. 6. OAE (between the estimated surface maps and the subset of reference ALT data used for scale identification) versus candidate scales for each investigated region.

semivariogram generated with the parameter set p_5 along with the best fitting model are given in Fig. 9(a) and Fig. 9(b), respectively. Fig. 9(d) and Fig. 9(e) report the same analysis performed on the samples of the bedrock at 4500m. As one can see by comparing Fig. 9(a) and Fig. 9(d), the bedrock has a much higher elevation variability at short range than the surface. This is also confirmed statistically (see Appendix A), since the surface is better modeled by the Gaussian model, see Fig. 9(b), whereas the bedrock is better modeled by the Exponential model, see Fig. 9(e). The identified best fitting models are then used to generate the surface and the bedrock elevation maps, which are reported in Fig. 9(c) and Fig. 9(f), respectively. The above analysis has been performed for all regions at the identified optimal scale. The obtained results, which are summarized in Tab. II, can be interpreted by analyzing the input data provided in Fig. 5 as follows:

- The surface typically has a smoother short range topography than the bedrock. Specifically, on all regions at the optimal scale the surface is modeled by the Gaussian model. The bedrock has a sharper short range variability on regions R1 and R2, at scales 3000 and 4500, where it is modeled by the Spherical and Exponential models, respectively, and a smoother variability on regions R3 and R4, at scales 7500 and 8500, respectively, where it

is modeled by the Gaussian model.

- The OU values of the surface (in the range ≈ 10 -16m) are much lower than the OU values of the bedrock (in the range ≈ 100 -170m), independently of the investigated region and identified optimal scale. This can be explained by the fact the the bedrock has a much higher variability than the surface.
- The minimum OU across parameter sets (see Tab. II) is obtained with different parameter sets on different regions at the optimal scale [e.g., on region R1 at scale 3000m, the best parameter set for estimating the ice surface map is p_8 , whereas on region R2 at scale 4500m the best parameter set is p_5 (see also Fig. 8)]. This confirms the importance of studying the dependence of the OK solution on the parameter set in order to obtain maps with the highest overall quality; on the contrary, the use of parameter sets different from those identified would result in estimates with lower overall quality.

Ice surface and bedrock maps are generated for all the investigated regions with the parameter sets and fitting models reported in Tab. II. The corresponding thickness maps are illustrated in Fig. 10. As one can see, apart from few errors mainly at the borders of the investigated regions (e.g., see the bottom right pixel on region R3 in Fig. 10), the obtained range of values of the ice thickness is similar to the range provided in the most recent compilation of ice thickness data, i.e., BEDMAP2 [7], over the Byrd Glacier. The main difference is that the BEDMAP2 ice thickness map is generated at an empirically derived scale of 5km (subsequently rendered at 1km to capture the complexity of mountainous areas [7]), whereas the results obtained here are generated at scales derived automatically, based on an objective statistical analysis of the variability of the surfaces and of the sampling of the RS, and validated with the ALT data. The scale of 5km (or 1km) used in BEDMAP2 is an acceptable compromise for gridding at a unique scale the whole Antarctica, although the RS sampling is extremely heterogeneous over the whole continent (see [7]). Because of this heterogeneous sampling, it is not expected that 5km (or 1km) is a optimal scale for interpolation in region R3, where the across-track sampling of the RS is relatively low, i.e., between ≈ 10 km and 30km. Conversely, the higher across-track sampling in R1, i.e., between ≈ 1 km and 5km, allows the generation of ice sheet maps with higher resolution than 5km.

Besides the qualitative assessment, we performed a quantitative validation of the obtained results. To this aim, we used a second subset of the reference ALT data, i.e., $S_V^{ALT}(s_j)$, $j = [1..J]$, which has been generated as explained in Sec. III-B1. The validation results are reported in Tab. III. As one can see, during the validation phase the minimum OAE values obtained on the four regions are very similar to those obtained during the scale identification phase. This confirms the robustness of the method to the identification of the optimal scale given the random choice of the reference ALT data. Note that on the one hand, the optimal scale identification and validation with the proposed method is possible for the interpolation of the surface due to the availability of ice surface ALT reference

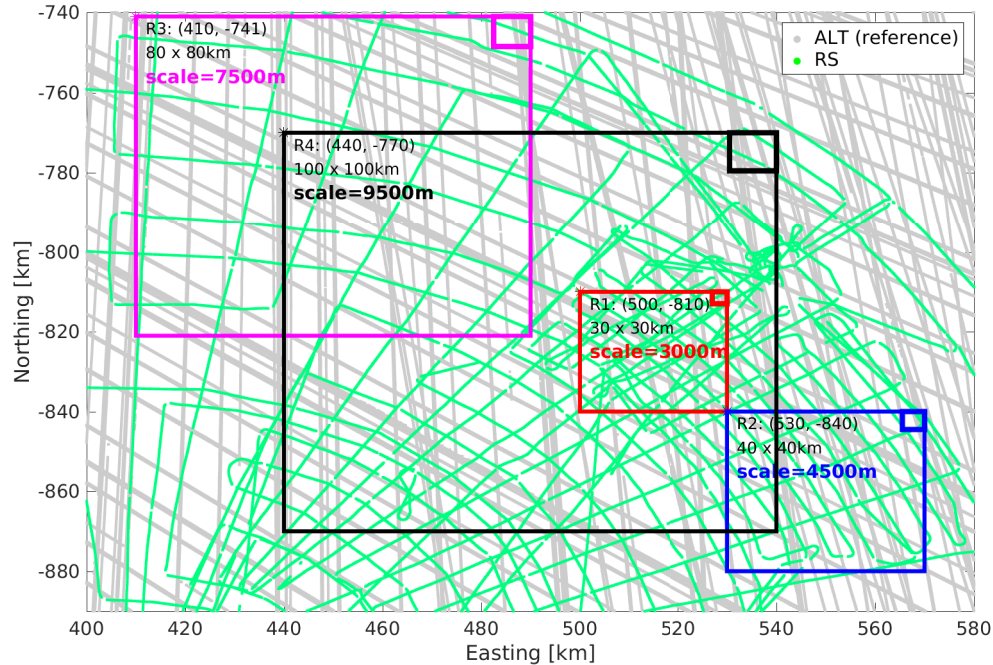


Fig. 7. Distribution of the RS and ALT sampling over the Byrd Glacier and identified optimal scale in each region. The dimension in km and the polar stereographic (70S latitude of true scale) (x,y) coordinates of the top left corner of each region are also illustrated. The top right rectangle in each region represents the size of the output grid maps at the identified optimal scale.

TABLE II

SUMMARY OF THE RESULTS OBTAINED FOR THE ESTIMATION OF THE SURFACE AND BEDROCK MAPS IN THE INVESTIGATED REGIONS OF THE BYRD GLACIER.

	Identified optimal scale	OAE	Surface		Bedrock	
			Best parameter set and related OU	Semivariogram fitting model	Best parameter set and related OU	Semivariogram fitting model
R1	3000m	11.82m	p8, OU = 13.86m	Gau	p3, OU = 110.43m	Sph
R2	4500m	40.57m	p5, OU = 10.97m	Gau	p8, OU = 168.77m	Exp
R3	7500m	58.97m	p5, OU = 15.97m	Gau	p5, OU = 153.10m	Gau
R4	8500m	24.13m	p5, OU = 12.74m	Gau	p7, OU = 102.14m	Gau

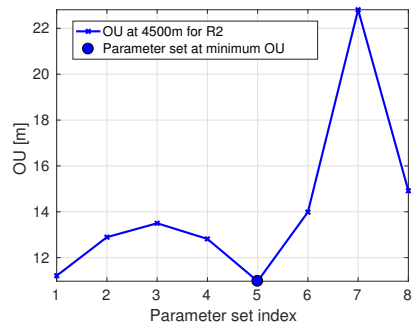


Fig. 8. OU variability across parameter sets for the estimated ice surface map of region R2 at scale 4500m.

data. On the other hand, the approach is general and could be analogously applied to identify and validate the optimal scale of the bedrock, when reference data for the bedrock will be available (e.g., 3D bed topography [29]).

TABLE III

SUMMARY OF THE RESULTS OBTAINED DURING THE SCALE IDENTIFICATION PHASE VERSUS THE SCALE VALIDATION PHASE.

	Scale identification phase		Validation phase	
	Obtained scale	OAE	Obtained scale	OAE
R1	3000m	11.82m	3000m	12.09m
R2	4500m	40.57m	4500m	39.90m
R3	7500m	58.97m	7500m	59.01m
R4	8500m	24.13m	8500m	24.16m

By analyzing together Fig. 7 and Fig. 10 one can understand the usefulness and effectiveness of the proposed technique for the identification of the optimal scale. For instance, in the regions R1, R2 and R3, the scales could be also qualitatively inferred as a compromise by empirically analyzing the sampling density. However, the method provides an objective scale that accounts for both the RS sampling and the ice surface topography. Note that without an objective and quantitative statistical analysis, the effect of the surface topography on the

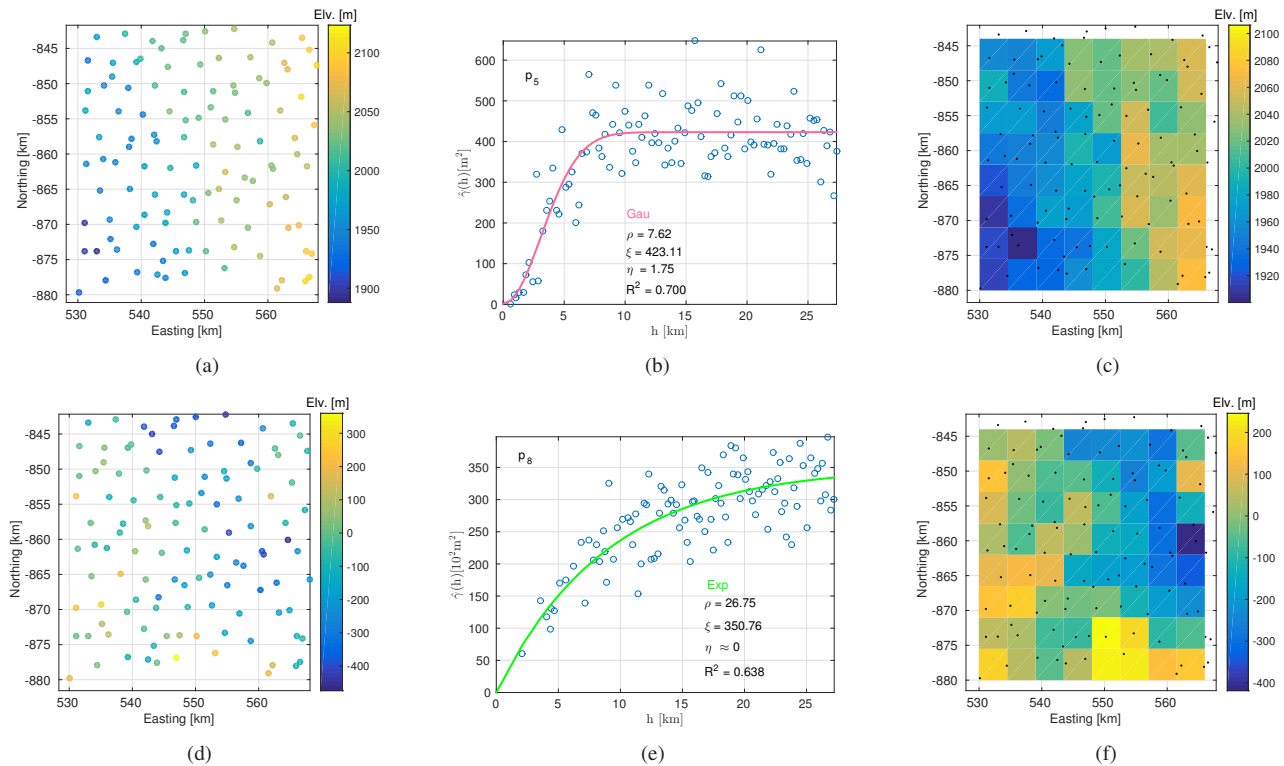


Fig. 9. (a) RS measurements of the surface at scale 4500m on region R2; (b) Corresponding semivariogram generated with the parameter set p_5 along with the best fitting model; and (c) Corresponding map of the ice surface at scale 4500m; (d) RS measurements of the bedrock at scale 4500m on region R2; (e) Corresponding semivariogram generated with the parameter set p_8 along with the best fitting model; and (f) Corresponding map of the bedrock at scale 4500m.

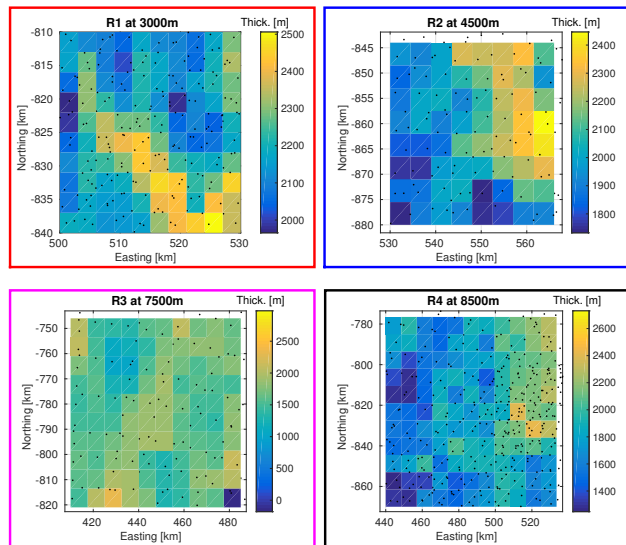


Fig. 10. Estimated ice thickness maps of the four investigated regions, R1, R2, R3 and R4 in the red, blue, magenta and black rectangles, respectively. The black dots represent the position of the rescaled RS data at the identified optimal scales, i.e., 3000m, 4500m, 7500, 8500m for the regions R1, R2, R3 and R4, respectively.

choice of the scale is difficult to quantify. Accordingly, the method becomes a valuable tool for the automatic 3D reconstruction of the ice sheet in areas characterized by variable RS sampling density, e.g., R4. The analysis of Fig. 7 and Fig. 10 also points out a potential disagreement on the estimated scales on overlapping regions, e.g., although region R1 is completely inside region R4, the estimated scales are 3000m and 8500m, respectively. This is because the criterion used for the identification of the optimal scale considers the overall surface variability and data sampling within the whole region. Thus, in the mentioned example, given that these characteristics are very different in the regions R1 and R4, it is reasonable that the optimal scales estimated by the proposed technique are also different. As a final remark, note that the method cannot avoid the generation of artifacts in areas with low sampling density and the generation of oversmoothed maps in areas with high sampling density. However, the method ensures that such negative effects have the lowest overall impact at the identified optimal scale over the whole investigated region compared to the maps that could be obtained at scales derived empirically.

V. CONCLUSION

This paper presents an automatic best-effort approach to reliably reconstruct the ice sheet geometry using RS data for interpolation and surface ALT data to derive and validate the scale (or grid size) for interpolation. In particular, while other methods in the literature interpolate the RS measurements at

a scale derived empirically from the qualitative analysis of the RS sampling, the presented method first analyzes statistically the sampling and the variability of the surfaces across different potential candidate scales. This is done with the OK method. Then the optimal scale is identified automatically and subsequently validated based on an objective criterion that compares the ice surface interpolation results obtained at different scales with two different subsets of samples drawn from the reference ALT data. It is worth noting that the method provides a single scale that is optimal for the entire region under investigation. In the absence of reference data of the bedrock, the optimal scale is then used for interpolating the bedrock measurements in order to generate scale-comparable maps that are subtracted in order to generate the ice thickness map. Hence, the scale is optimal for the interpolation of the surface, whereas it is coherent and likely suboptimal, but reasonably chosen, for the estimation of the bedrock map. For this reason, the method is a best-effort approach to the reconstruction of the ice sheet geometry, in the presence of the ALT ice surface data and in the absence of bedrock reference data. Moreover, at the optimal scale, the method provides the ice surface and bedrock maps having the minimum overall uncertainty with respect to the choice of OK parameter values.

The method has been applied to airborne RS data acquired by MCoRDS and satellite ALT data acquired by GLAS over a portion of the Byrd Glacier in Antarctica. The topography of the ice surface and the RS sampling within the investigated portion vary considerably. Thus, in order to prove the effectiveness of the method for the automatic identification of the scale, we applied it locally to four regions that are different in terms of area, topography variation and RS sampling. From the analysis of the results it appears that the obtained scales are appropriate given the characteristics of the input data. These have also been compared qualitatively with the scales provided by other methods, i.e., BEDMAP2, over the same region. The multiple scales provided by our method are tuned to the investigated scenarios in that our method accounts for the regional topography and sampling of the RS data. In contrast, BEDMAP2 has been generated for the whole Antarctica at a scale which is derived empirically and appears to be a compromise given the extremely heterogeneous RS sampling over the whole continent. We also performed a quantitative validation of the results by using a second subset of ALT data. The quantitative analysis points out the robustness of the method to the random choice of the reference ALT data. The validation phase confirms that the identified optimal scales are typically larger than those desired for specific science requirements. However, this should not be regarded as a weakness of the method, rather as an effect of the poor data coverage. In this case, the method can be used as a guideline for future RS surveys. Indeed, a possible strategy to reduce the scale for interpolation is the planning of campaigns with more dense RS flightlines. If this is impractical due to logistical constraints, the analysis of the results provided by the method offers the possibility to perform a quantitative error assessment at scales that match the needs of specific objectives or applications (e.g., ice sheet modeling), but are different from the optimal scale. Furthermore, it enables evaluating the

criticality in choosing arbitrarily the scales for interpolation.

It is important to note that the described method can be applied to smooth, rough and more generally to any kind of surface, and the obtained results capture this topography variability. This is enabled by the intrinsic advantage of the OK method that quantifies statistically the variability of the data prior to the interpolation. As such, we derived that, at the identified optimal scales, the topography of the surface (always modeled by a Gaussian function) is typically smoother than that of the bedrock (modeled by either the Spherical, Exponential or Gaussian functions, depending on the region). This is expected since the study area is the Byrd Glacier, which lies near the Transantarctic Mountains, where the bedrock presents a steep relief. Also, this is qualitatively confirmed by investigating the short range variability on the surface and bedrock directly from the RS measurements.

The OK method can be run with different combinations of parameters, i.e., parameter sets, which provide different OK solutions, i.e., couples of estimated and uncertainty maps. In this paper we performed an analysis of the OK method performance across parameter sets and observed that at the identified optimal scales, for the different regions there are different parameter sets that provide the maps with the highest overall quality. This highlights the importance of such analysis when high quality interpolation maps are desired. If there are no stringent requirements on the quality of the interpolation, in order to reduce the complexity of the method, any of the discussed parameter sets can be used at the expense of a loss in quality (e.g., Fig. 8 shows that for the R2 region the overall uncertainties of the estimated ice surface maps vary from a minimum of $\approx 13\text{m}$ obtained with p_5 to a maximum of $\approx 22\text{m}$ obtained with p_7). The analysis of the results also points out that independently on the region, the overall uncertainty on the surface is about one order of magnitude lower than that on the bedrock, i.e., in the range 10-20m and 100-200m for the surface and bedrock, respectively. This can be explained again by the smoother topography of the surface with respect to the topography of the bedrock. A possible solution for the reduction of the high uncertainty at the bedrock could be a better RS sampling of the surveyed region.

By comparing the final surface, bedrock and thickness maps across the investigated regions, one can see that in regions with uniform sampling density, although the scale could be qualitatively inferred, the method provides a scale that accounts both for the sampling and also surface topography, whose effect on the scale is difficult to qualitatively assess. Furthermore, the method is a valuable tool for the automatic 3D reconstruction of the ice sheet geometry in areas characterized by variable RS sampling density as it interpolates the RS measurements at a scale that minimizes the overall errors with respect to the available ice surface reference ALT data. Moreover, note that when reference data of the bedrock will be available, the method could be applied to the identification and validation of the optimal scale for the interpolation of the bedrock, offering the possibility to improve current estimates in glaciology, e.g., ice sheet volume.

As future developments of this research, we plan to study the possibility to refine the estimated 3D maps by including in

the method possible known input data uncertainties and their effects on the results provided by the adopted geostatistical interpolation strategy. Moreover, we aim to extend the method by including the modeling of possible anisotropic behavior of the ice sheets.

VI. ACKNOWLEDGEMENTS

This research has been funded by the Italian Space Agency (ASI) under the framework of "SaTellite Radar sounder for eArTh sUb-surface Sensing (STRATUS)", contract ASI N. ASI 2016_14_U.O. We acknowledge the use of data and/or data products from CReSIS generated with support from NSF grant ANT-0424589 and NASA grant NNX10AT68G. The authors would like to thank the anonymous reviewers for the useful suggestions that helped improving the manuscript.

APPENDIX

In this Appendix, background notions about the OK interpolation method are provided (for a detailed study of the OK method the reader is referred to [22], [31], [32]).

OK is a geostatistical interpolation method that estimates the value of a random variable at an query position x_0 , i.e., $\hat{e}(x_0)$, based on N_0 known/observed values at neighboring positions $x_n, n = [1..N_0]$, i.e., samples $e(x_n)$ in the domain of interest. OK relies on what is called spatial variability analysis (SVA), which is a process that analyzes statistically the variability of the investigated surfaces by quantifying the spatial autocorrelation of the available samples. This is done through the generation and model fitting of the empirical semivariogram $\hat{\gamma}(\mathbf{h})$. Here we assume an isotropic model of spatial variability (a more complex analysis relies on the assumption of anisotropic models of spatial variability [31]). Under this assumption $\hat{\gamma}(\mathbf{h})$ is a graph generated by computing the squared difference between all pairs of samples separated by a distance (lag) h_k . \mathbf{h} is the vector of point pair distances h_k , with $k = [1..\bar{k}]$, where \bar{k} is the maximum number of bins of the semivariogram. Depending on the application domain, several candidate theoretical parametric models γ^{Can} can be used to fit the empirical semivariogram. Here below we report the analytical formulation of the theoretical models used in our analysis, i.e., the Spherical γ^{Sph} , Exponential γ^{Exp} , Gaussian γ^{Gau} and Linear γ^{Lin} models.

- The Spherical model:

$$\gamma^{Sph}(h; \theta) = \begin{cases} 0, & h = 0, \\ \eta + (\xi - \eta) \left[\frac{3}{2} \cdot \frac{h}{\rho} - \frac{1}{2} \left(\frac{h}{\rho} \right)^3 \right], & 0 < h \leq \rho, \\ \xi, & h > \rho, \end{cases} \quad (2)$$

- The Exponential model:

$$\gamma^{Exp}(h; \theta) = \begin{cases} 0, & h = 0, \\ \eta + (\xi - \eta) \left[1 - e^{-\frac{3h}{\rho}} \right], & h > 0, \end{cases} \quad (3)$$

- The Gaussian model:

$$\gamma^{Gau}(h; \theta) = \begin{cases} 0, & h = 0, \\ \eta + (\xi - \eta) \left[1 - e^{-\frac{3h^2}{\rho^2}} \right], & h > 0. \end{cases} \quad (4)$$

$\theta = (\rho, \xi, \eta)$ is the vector of parameters of these models, where the range ρ is the distance after which the samples lose spatial correlation, the sill ξ is the value that the semivariogram has at ρ , and the nugget η is associated with measurement errors and variations at microscales smaller than the distances between the available samples.

- The Linear model:

$$\gamma^{Lin}(h; \theta) = \begin{cases} 0, & h = 0, \\ \eta + bh, & h > 0, \end{cases} \quad (5)$$

where b is the slope and η is the value of the semivariogram where the line fitted to the data intersects the y-axis.

We chose these models since they are legitimate for fitting semivariograms [31] and are likely to fit elevation data [31] (e.g., the Exponential and Linear models have been used in [10] for the 3D reconstruction of the ice sheet). In particular, the Spherical and Exponential models have a steep behavior near the origin, and therefore are suitable for representing surfaces with high elevation variability at short range, i.e., with weak autocorrelation. Among the two models, the Exponential model, with its steeper behaviour near the origin, is appropriate for representing rougher surfaces. The Gaussian model has a parabolic shape near the origin, therefore it is suitable for representing smoothly varying surfaces [31]. The Linear model indicates non-stationarity in the data. The presence of non-stationarity in the data invalidates the intrinsic hypothesis required in geostatistics. A common approach to solve the problem of non-stationarity is to fit a trend surface to the data, to regenerate the semivariogram by using the residuals [31], [33] and repeat the fitting procedure, which is described here below.

The vector of parameters θ of each theoretical model can be estimated on the basis of the weighted least square criterion [34], expressed as follows:

$$\tilde{\theta} = \min_{\theta} \sum_{k=1}^{\bar{k}} w_k [\hat{\gamma}(h_k) - \gamma^{Can}(h_k, \theta)]^2, \quad (6)$$

where w_k is the weight associated to bin k . Then, the fitting performances of these models can be quantified in terms of the R^2 indicator; the best fitting model with the associated vector of parameters $\gamma^*(\mathbf{h}; \tilde{\theta})$ is the one that maximizes R^2 . $\gamma^*(\mathbf{h}; \tilde{\theta})$ is the output of the SVA and is used to interpolate the observed samples in order to estimate $\hat{e}(x_0)$. Moreover, since OK is a (geo)statistical method, it also provides an uncertainty value $u(x_0)$ associated with $\hat{e}(x_0)$ (for the analytic formulation of $\hat{e}(x_0)$ and $u(x_0)$ the reader is referred to [22], [32]). On the basis of the couple of estimates $\hat{e}(x_0)$ and $u(x_0)$, one can infer with 95% confidence that the true value $e(x_0)$ lies in the interval $[\hat{e}(x_0) \pm u(x_0)]$ [32]. Therefore, the lower the uncertainty value, the more the estimated value is expected to approach the true value, i.e., the better the estimation.

SVA can be performed by choosing the way of constructing the semivariogram (i.e., the way of creating the

bins of the semivariogram [32]) and also by choosing the way the semivariogram fitting model is weighted [35]. In other words, depending on these choices, SVA can be performed by using different combinations of *binning* the semivariogram and *weighting* the fitting model. Since the dependence of the OK solution on these combinations (or parameter sets $p_i, i = [1..P]$) has not been sufficiently investigated in the scenario of the 3D reconstruction of the ice sheets, we here study several possible parameter sets (see Tab. IV). In particular, we study the two possible ways to perform the *binning* of the semivariogram depending on the aggregation of point pairs in each bin, i.e., constant binsize (bs) and constant binwidth (bw). In both cases, h_k is computed as the mean value of all the distances inside bin k . With the bs option, we create bins (of point pair distances) with variable width and with constant number of point pairs within each bin. In the bw option, the number of point pairs within each bin can vary, whereas the width of all \bar{k} bins is the same. Thus, $\text{binning} = \{\text{bw}, \text{bs}\}$ is the first subset of parameters within the OK parameter set (see Tab. IV). Furthermore, we consider the choice of the *weighting* function [see (6)] as the second subset of parameters of the OK method. The semivariogram weighting models that we identified in the literature [35] and used in our analysis are:

- **W1** = $\{w_k = 1, \forall k = [1..\bar{k}]\}$. This represents the case in which the weights are all constant, as for the ordinary least squares criterion.
- **W2** = $\{w_k = |N_k|, \forall k = [1..\bar{k}]\}$. In this case higher weight is given to the bins k containing a higher number of samples N_k .
- **W3** = $\{w_k = 1/[\gamma(h_k; \theta)]^2, \forall k = [1..\bar{k}]\}$. This is a particular case of inverse distance weighting, in which the experimental variogram points close to the origin receive higher weight than experimental variogram points at larger distances.
- **W4** = $\{w_k = |N_k|/[\gamma(h_k; \theta)]^2, \forall k = [1..\bar{k}]\}$. In this case the weights are set to the inverse of the uncertainty of the semivariogram estimate (or estimation variance). This is a popular weighting function [34], proven to work in many practical situations as it represents a good compromise of statistical efficiency and computability.
- **W5** = $\{w_k = |N_k|/h_k^2, \forall k = [1..\bar{k}]\}$. This weighting function gives more weight to estimates calculated with more point pairs and at short distances [36].

Therefore, $\text{weighting} = \{\mathbf{W1}, \mathbf{W2}, \mathbf{W3}, \mathbf{W4}, \mathbf{W5}\}$ is the second subset of parameters within the OK parameter set (see Tab. IV). Considering all the combinations $\{\text{binning}, \text{weighting}\}$, one can deduce that there are 10 possible parameter sets p_i for the semivariogram best model fitting. In fact, note that the number of parameter sets reduces to $P = 8$ (see Tab. IV), since by definition, the parameter set $\{\text{bs}, \mathbf{W1}\} \equiv \{\text{bs}, \mathbf{W2}\}$, and $\{\text{bs}, \mathbf{W3}\} \equiv \{\text{bs}, \mathbf{W4}\}$. Given the parameter sets, it is worth to highlight the dependence of the fit on p_i ; there

are P semivariogram best fitting models $\gamma_{p_i}^*(\mathbf{h}; \tilde{\theta}), i = [1..P]$, each characterized by different values of the vector of parameters $\tilde{\theta}$. It is then straightforward that for a query point x_0 , not a single couple of estimates $\hat{e}(x_0)$ and $u(x_0)$, but P couples of estimates $\hat{e}^i(x_0)$ and $u^i(x_0), i = [1..P]$, can be generated. By extending this reasoning to all the query points in the domain of interest, the OK method provides P couples of estimated elevation and uncertainty maps.

TABLE IV
PARAMETER SETS CONSIDERED IN THE OK METHOD.

binning	weighting	parameter set
bw	W1 = $\{w_k = 1\}$	$p_1 = \{\text{bw}, \mathbf{W1}\}$
bs	W2 = $\{w_k = N_k \}$	$p_2 = \{\text{bw}, \mathbf{W2}\}$
	W3 = $\{w_k = 1/[\gamma(h_k; \theta)]^2\}$	$p_3 = \{\text{bw}, \mathbf{W3}\}$
	W4 = $\{w_k = N_k /[\gamma(h_k; \theta)]^2\}$	$p_4 = \{\text{bw}, \mathbf{W4}\}$
	W5 = $\{w_k = N_k /h_k^2\}$	$p_5 = \{\text{bw}, \mathbf{W5}\}$
		$p_6 = \{\text{bs}, \mathbf{W1}\}$
		$p_7 = \{\text{bs}, \mathbf{W3}\}$
		$p_8 = \{\text{bs}, \mathbf{W5}\}$

REFERENCES

- [1] A. Shepherd, E. Ivins, A. Geruo, V. Barletta, M. J. Bentley, S. Bettadpur, K. Briggs, D. Bromwich, R. Forsberg, N. Galin *et al.*, "A reconciled estimate of ice-sheet mass balance," *Science*, vol. 338, no. 6111, pp. 1183–1189, 2012.
- [2] A. Payne, "A thermomechanical model of ice flow in West Antarctica," *Climatic Dynamics*, vol. 15, no. 2, pp. 115–125, 1999.
- [3] S. Riedel and D. Jokat, W. and Steinhage, "Mapping tectonic provinces with airborne gravity and radar data in Dronning Maud Land, East Antarctica," *Geophysical Journal International*, vol. 189, no. 1, pp. 414–427, 2012.
- [4] N. Holschuh, D. Pollard, R. Alley, and S. Anandakrishnan, "Evaluating Marie Byrd Land stability using an improved basal topography," *Earth and Planetary Science Letters*, vol. 408, pp. 362 – 369, 2014.
- [5] D. Vaughan, J. Comiso, I. Allison, J. Carrasco, G. Kaser, R. Kwok, P. Mote, O. Solomina, K. Steffen, and T. Zhang, "Observations: Cryosphere," In: *Climate Change 2013: The Physical Science Basis. Contribution of Working Group I to the Fifth Assessment Report of the Intergovernmental Panel on Climate Change*, 2013.
- [6] M. Lythe and D. Vaughan, "BEDMAP: A new ice thickness and subglacial topographic model of Antarctica," *Journal of Geophysical Research: Solid Earth*, vol. 106, no. B6, pp. 11 335–11 351, 2001.
- [7] P. Fretwell *et al.*, "Bedmap2: improved ice bed, surface and thickness datasets for Antarctica," *The Cryosphere*, vol. 7, no. 1, pp. 375–393, 2013.
- [8] J. Bamber, "A new ice thickness and bed data set for the Greenland ice sheet 1. Measurement, data reduction, and errors," *J. Geophys. Res.*, vol. 106, no. 33, pp. 773–33, 2001.
- [9] J. Bamber, J. Griggs, R. Hurkmans, J. Dowdeswell, S. Gogineni, I. Howat, J. Mouginot, J. Paden, S. Palmer, E. Rignot, and D. Steinhage, "A new bed elevation dataset for Greenland," *The Cryosphere*, vol. 7, no. 2, pp. 499–510, 2013.
- [10] K. Lindbäck, R. Pettersson, S. Doyle, C. Helanow, P. Jansson, S. Kristensen, L. Stenseng, R. Forsberg, and A. Hubbard, "High-resolution ice thickness and bed topography of a land-terminating section of the Greenland Ice Sheet," *Earth System Science Data*, vol. 6, no. 2, pp. 331–338, 2014.
- [11] S. Gogineni, J. Yan, J. Paden, C. Leuschen, J. Li, F. Rodriguez-Morales, D. Braaten, K. Purdon, Z. Wang, W. Liu, and J. Gauch, "Bed topography of Jakobshavn Isbrae, Greenland, and Byrd Glacier, Antarctica," *Journal of Glaciology*, vol. 60, no. 223, pp. 813–833, 2014.
- [12] M. Huss and D. Farinotti, "Distributed ice thickness and volume of all glaciers around the globe," *Journal of Geophysical Research: Earth Surface (2003–2012)*, vol. 117, no. F4, 2012.
- [13] —, "A high-resolution bedrock map for the Antarctic Peninsula," *The Cryosphere*, vol. 8, no. 4, pp. 1261–1273, 2014.

- [14] J. Roberts, R. Warner, D. Young, A. Wright, T. van Ommen, D. Blankenship, M. Siegert, N. Young, I. Tabacco, A. Forieri, A. Passerini, A. Zizzotti, and M. Frezzotti, "Refined broad-scale sub-glacial morphology of Aurora Subglacial Basin, East Antarctica derived by an ice-dynamics-based interpolation scheme," *The Cryosphere*, vol. 5, no. 3, pp. 551–560, 2011.
- [15] R. Warner and W. Budd, "Derivation of ice thickness and bedrock topography in data-gap regions over Antarctica," *Annals of Glaciology*, vol. 31, no. 1, pp. 191–197, 2000.
- [16] D. Rippin, J. Bamber, M. Siegert, D. Vaughan, and H. Corr, "Basal topography and ice flow in the Bailey/Slessor region of East Antarctica," *Journal of Geophysical Research: Earth Surface*, vol. 108, no. F1, 2003.
- [17] M. Morlighem, E. Rignot, H. Seroussi, E. Larour, H. Ben Dhia, and D. Aubry, "A mass conservation approach for mapping glacier ice thickness," *Geophysical Research Letters*, vol. 38, no. 19, 2011.
- [18] M. Morlighem, E. Rignot, J. Mouginot, H. Seroussi, and E. Larour, "High-resolution ice-thickness mapping in South Greenland," *Annals of Glaciology*, vol. 55, no. 67, pp. 64–70, 2014.
- [19] G. Durand, O. Gagliardini, L. Favier, T. Zwinger, and E. Le Meur, "Impact of bedrock description on modeling ice sheet dynamics," *Geophysical Research Letters*, vol. 38, no. 20, 2011.
- [20] J. Goff, E. Powell, D. Young, and D. Blankenship, "Conditional simulation of Thwaites Glacier (Antarctica) bed topography for flow models: incorporating inhomogeneous statistics and channelized morphology," *Journal of Glaciology*, vol. 60, no. 222, pp. 635–646, 2014.
- [21] F. Graham, J. Roberts, B. Galton-Fenzi, D. Young, D. Blankenship, and M. Siegert, "A high-resolution synthetic bed elevation grid of the Antarctic continent," *Earth System Science Data*, vol. 9, no. 1, pp. 267–279, 2017.
- [22] N. Cressie, *Statistics for spatial data*. Wiley series in probability and mathematical statistics. J. Wiley & Sons, 1993.
- [23] F. Rodriguez-Morales, S. Gogineni, C. Leuschen, J. Paden, J. Li, C. Lewis, B. Panzer, D. Gomez-Garcia Alvestegui, A. Patel, K. Byers, R. Crowe, K. Player, R. Hale, E. Arnold, L. Smith, C. Gifford, D. Braaten, and C. Panton, "Advanced multifrequency radar instrumentation for Polar Research," *IEEE Transactions on Geoscience and Remote Sensing*, vol. 52, no. 5, pp. 2824–2842, May 2014.
- [24] H. J. Zwally, R. Schutz, C. Bentley, J. Bufton, T. Herring, J. Minster, J. Spinhirne, and R. Thomas, "GLAS/ICESat L2 Antarctic and Greenland Ice Sheet Altimetry Data, Version 34. Boulder, Colorado USA. NASA National Snow and Ice Data Center Distributed Active Archive Center." <https://nsidc.org/data/GLA12/versions/34>, 2014.
- [25] M. Peters, D. Blankenship, and D. Morse, "Analysis techniques for coherent airborne radar sounding: Application to West Antarctic ice streams," *Journal of Geophysical Research: Oceans*, vol. 110, no. 6, pp. 1–17, 2005.
- [26] C. Hernandez, V. Krozer, J. Vidkjaer, and J. Dall, "POLARIS: ESA's airborne ice sounding radar front-end design, performance assessment and first results," in *Microwave Symposium Digest, 2009. MTT '09. IEEE MTT-S International*, June 2009, pp. 393–396.
- [27] A.-M. Ilisei and L. Bruzzone, "A system for the automatic classification of ice sheet subsurface targets in radar sounder data," *IEEE Transactions on Geoscience and Remote Sensing*, vol. 53, no. 6, pp. 3260–3277, 2015.
- [28] J. Li, J. Paden, C. Leuschen, F. Rodriguez-Morales, R. Hale, E. Arnold, R. Crowe, D. Gomez-Garcia, and P. Gogineni, "High-altitude radar measurements of ice thickness over the Antarctic and Greenland ice sheets as a part of Operation IceBridge," *IEEE Transactions on Geoscience and Remote Sensing*, vol. 51, no. 2, pp. 742–754, 2013.
- [29] J. Paden, T. Akins, D. Dunson, C. Allen, and P. Gogineni, "Ice-sheet bed 3-D tomography," *Journal of Glaciology*, vol. 56, no. 195, pp. 3–11, 2010.
- [30] J. DiMarzio, "GLAS/ICESat 500 m Laser Altimetry Digital Elevation Model of Antarctica," 2007.
- [31] G. Bohling, "Introduction to geostatistics and variogram analysis," 2005.
- [32] T. Smith, "Notebook on spatial data analysis," <http://www.seas.upenn.edu/~ese502/#notebook>, year = 2016,.
- [33] S. Vieira, R. Carvalho, de Josa, M. Ceddia, and A. Gonzalez, "Detrending non stationary data for geostatistical applications," *Bragantia*, vol. 69, pp. 01 – 08, 2010.
- [34] N. Cressie, "Fitting variogram models by weighted least squares," *Journal of the International Association for Mathematical Geology*, vol. 17, no. 5, pp. 563–586, 1985.
- [35] E. Pardo-Iguzquiza, "VARFIT: a fortran-77 program for fitting variogram models by weighted least squares," *Computers and Geosciences*, vol. 25, no. 3, pp. 251–261, 1999.
- [36] X. Zhang, J. Van Eijkeren, and A. Heemink, "On the weighted least-squares method for fitting a semivariogram model," *Computers and Geosciences*, vol. 21, pp. 605–608, May 1995.